MATERIALS FOR ELECTROCHEMICAL

CELL SEPARATORS

SECOND SUMMARY REPORT

3 JULY 1967

N67-30685
(ACCESSION NUMBER) _____ (THRU)
FACILITY FORM

_____ (PAGES) _____ (CODE)

CR-72267 _____ 03
(NASA CR OR TMX OR AD NUMBER) _____ (CATEGORY)

Prepared for:

NATIONAL AERONAUTICS AND SPACE ADMINISTRATION
LEWIS RESEARCH CENTER
Under Contract NAS 3-8522

TRW EQUIPMENT LABORATORIES

CLEVELAND, OHIO

NAS CR-72267

Second Summary Report

MATERIALS FOR ELECTROCHEMICAL CELL SEPARATORS

Prepared by

J. W. Vogt

for

National Aeronautics and Space Administration

3 July 1967

Contract No. NAS 3-8522

Technical Management

NASA - Lewis Research Center
Electrochemical Systems Branch
Daniel G. Soltis

Materials Technology
TRW Equipment Laboratories
TRW Inc.
23555 Euclid Avenue
Cleveland, Ohio 44117

I FOREWORD

This report is the Summary Report on Task 2 of Contract NAS 3-8522 and describes work performed during the January to June 1967 time period. This contract is concerned with developing improved materials for use as electrochemical cell separators. Task 1 of the program dealt with determining the properties of "Fuel Cell Grade Asbestos" separator mats. Task 2 of the program has been the study of other types of asbestoses and alternate inorganic fibrous materials. The scope of the original contract has now been extended to include a second year's work. This follow-on work will consist of studying composite mats incorporating fibrous forms of organic materials to add structural integrity to the most compatible inorganic materials uncovered in this program.
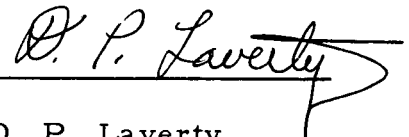
The NASA technical director for this contract is Daniel G. Soltis. We wish to acknowledge him for his help and cooperation during the course of this work. For internal control purposes, this report has been assigned the TRW Report Number ER 7055-3.

Prepared by _____

J. W. Vogt
Principal Engineer

Approved by _____

D. P. Laverty
Section Manager

Approved by _____

G. J. Guarnieri
Manager, Materials
Research and Development

II   TABLE OF CONTENTS

III INTRODUCTION

Purpose of the Program

As alkaline fuel cells and electrochemical cells have reached the present level of service expectancy, many vexing problems have been encountered and solved. With each successful extension of service life, formerly satisfactory components have limitations that represent obstacles to continued progress. The electrolyte matrix (or electrode separator) is now one significant obstacle to progress.

During the earlier stages of fuel cell development, chrysotile mat, available from Johns Manville Corporation as Fuel Cell Asbestos, was an adequate cell separator to permit tests of performance that were limited by failure of other parts. However, chrysotile is slowly dissolved by KOH electrolyte, and the appearance of constituent elements in the electrolyte and perhaps on the electrode surface is suspected as a contributing cause of slow decline in cell performance. Therefore, the search for a better matrix material has been undertaken as the primary goal of this program.

Desirable Properties of a Cell Matrix

The matrix of a cell has several important functions:

a) to provide physical separation and electrical insulation between electrodes,

b) to absorb and retain electrolyte,

c) to form a positive gas barrier between the electrodes, and

d) to provide a region of high electrolytic conductivity between the electrodes.

Chrysotile asbestos, being a soft, highly porous and wetting fibrous material, meets these requirements very well. Moreover, chrysotile mats are somewhat flexible and strong, and can therefore be handled easily when in the dry condition. The Arizona chrysotile, from which Fuel Cell Asbestos paper and board are made, is nearly-pure hydrated magnesium silicate which may be used without the extensive purification required to remove heavy metal impurities.

Because of the superiority of chrysotile among the materials available, it has been used widely in alkaline electrochemical cells, and consequently its performance is known in detail. It is naturally the material of choice to serve as a reference against which to evaluate other matrix materials.

Test Program

One goal of this program is to establish a small group of laboratory tests by which the performance of a prospective matrix material might be accurately predicted without recourse to complete cell tests. The tests selected for use in this program were intended to yield quantitative evaluation of properties closely related to the matrix function, and yet, at the same time, they were chosen to be as simple as possible.

The material of the matrix was examined for composition, fiber structure, surface area, and compatibility with KOH electrolyte. Dry mats in specified thicknesses were tested for tensile strength, porosity, density, thickness variation, and pore size distribution. Mats, wet with 30% KOH solution, were tested for electrolyte absorption, electrolyte retention under 25g acceleration, electrolytic resistance, gas permeability and electrochemical reactivity. The experimental details of these tests are described in the Task 1 summary report of this program* in regard to their application to the Fuel Cell Asbestos mats.

Materials Tested

Following the testing of chrysotile Fuel Cell paper and board, the same tests have been applied to other asbestoses, natural and chemically-modified. These are tremolite, anthophyllite, amosite, and crocidolite. They were modified by leaching with acids, wetting agents, or sequestering agents. Treatment with acid or sequestering agents was intended to remove the heavy metal constituents which may be transfered to electrode surfaces. The wetting agent was intended to promote separation of fibers, thus improving the mat properties.

In addition to these natural fibers, the tests were applied also to zirconia, hydrated magnesia, potassium titanate fiber (PKT), zirconium silicate, titanium oxide, silicon carbide, and ceria.

---

* J. W. Vogt; NAS CR-72148, "Study of Asbestos for Electrochemical Cells"; First Summary Report, Contract NAS 3-8522, TRW Inc., Dec. 28, 1966.

All these materials were first evaluated mainly on the basis of chemical compatibility with hot KOH. The four best materials were then formed into mats for the remainder of the test program.

This report briefly summarizes the properties of the Fuel Cell Grade Asbestos separators (as determined in Task 1 of the program) and compares these with the other candidate materials tested in the present phase (Task 2) of the program.

IV   SUMMARY OF ASBESTOS MAT PROPERTIES

Task 1 of this program consisted of testing Fuel Cell Asbestos, with the following general results reported in the Task 1 Summary Report:

1.   Tensile strength of the dry 20-mil thick paper is about 150 psi and seems to be reasonably constant within a production batch. The 60-mil thick millboard varied from tensile strengths of 80 to 170 psi within a production batch, with very marked differences between specimens taken from beginning and end of a production batch.

   During tensile testing of the 60-mil millboard specimens taken parallel to the processing direction underwent about twice the elongation as those specimens taken in the transverse direction. The 20-mil paper evidently does not have a similar directional dependency.

2.   Surface area, determined by nitrogen adsorption, is about 50 m^2/g

3.   Density, determined by the air comparison pycnometer, is 2.73 g/cc. Comparing this with the apparent density based on geometric volume, the dry paper is about 66% porous and the millboard is about 70% porous.

4.   Pore size distribution by the mercury intrusion method could not be measured. Evidently the porous chrysotile fibers collapsed under the mercury pressure and the pressure-volume profile was simply that of a continuously compressible solid.

5.   Electrolyte absorption and retention. The 60-mil millboard absorbs about 5.65 times its weight of 40% KOH solution, and retains about 72% of that solution during the 25 g acceleration test. The 20-mil paper does not swell as freely. It asborbs about 3.8 times its weight of 40% KOH and retains about 99% of this under the 25g test.

6. <u>Gas Permeability</u> was measured for the material both in the dry state and while containing KOH solution in various electrolyte-matrix weight proportions from 1 : 1 to saturation. The permeability rate for the dry specimen is evidently of little significance. When wetted with KOH, the 20-mil chrysotile paper consistently leaked gas even when saturated, at about 5 psi pressure differential. In contrast, the 60-mil millboard remained gas tight at 30 psi even at the 1 : 1 weight proportion of KOH solution.

7. <u>Electrolytic Resistance</u>. The apparatus used for these early tests permitted the specimen to swell without restraint, and the tests are, therefore, of dubious quantitative value. However, they do reveal, as do several other of the tests, that the paper specimens are more consistent than the millboard specimens. The millboard averaged about 0.84 ohm cm^2 (5.5 ohm cm); the paper about 0.47 ohm cm^2 (9 ohm cm).

8. <u>Chemical degradation</u> tests revealed that chrysotile, a hydrated magnesium silicate, reacts slowly with hot KOH solution by dissolution of the silicate constituent. The residual hydrated magnesium oxide is insoluble, but it is a gelatinous material completely lacking the fibrous character of the chrysotile. There was some indication that the fiber destruction was not general, but selective. At the end of the test, many fibers, apparently essentially unchanged, remained in the mass (Figure 1). However, at the end of a more severe test, all evidence of fibrous character had completely disappeared.

9. <u>Electrochemical Reactivity</u>. After 72 hours of exposure in 40% KOH at 100°C, to an electrolytic current density of 100 ASF, the electrolyte had apparently not acquired a significant quantity of constituent elements from the specimen. The anode surface became slightly mottled and the deposit proved to be iron - probably as the hydrated oxide.
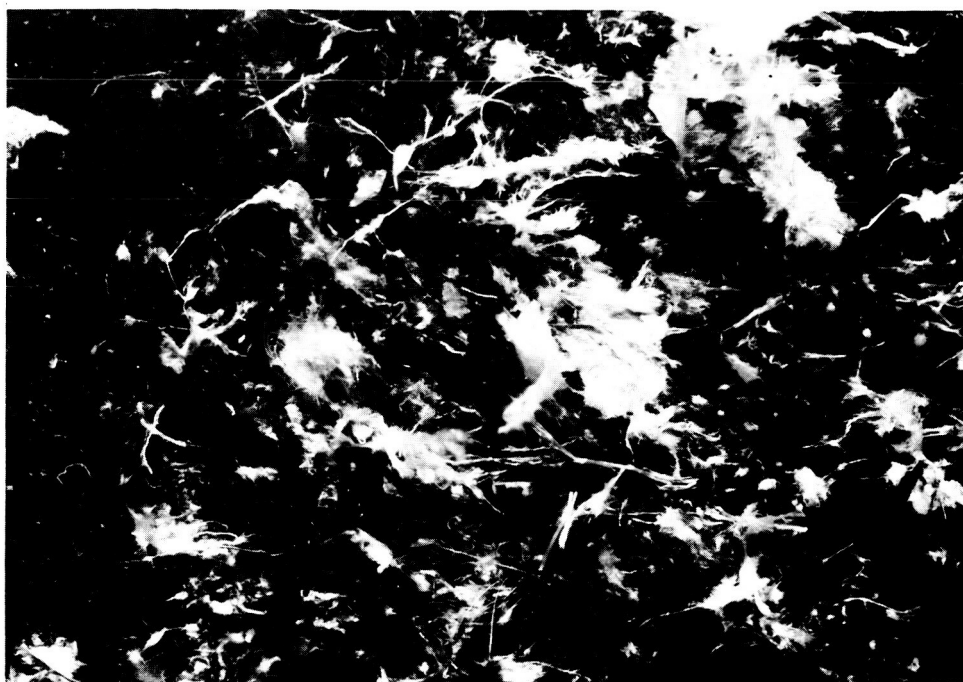
(a)
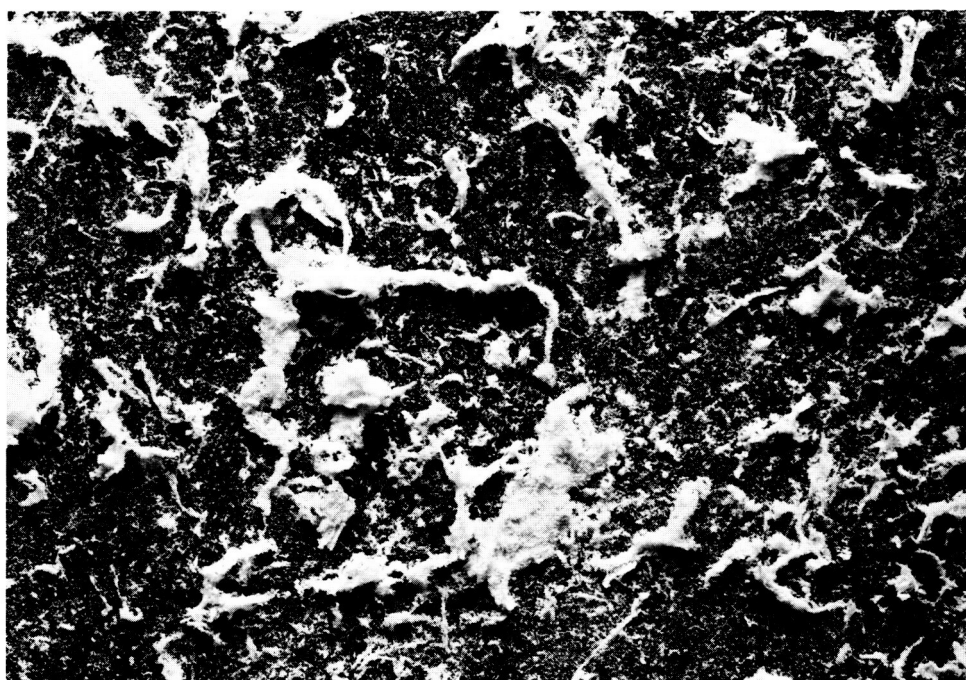
(b)

Figure 1.   Chrysotile (a) before and (b) after chemical degradation
            test.   Magnification 10X.

V SCREENING TESTS OF CANDIDATE MATERIALS

The additional materials being considered for use on this program beyond those evaluated in Task 1 were first tested by a chemical degradation test in order to determine which were the most promising to form into mats for further evaluation.

For this test, specimens were submerged in positively sealed containers (Figure 2) for 100 and 1000 hours in 30% and 50% KOH solution at 100°C and 150°C. Although this does not comprise the entire span of concentrations and temperatures specified for the program, it proves adequate to distinguish between the materials of possible value and the obvious failures.

The test was applied individually to:

> Tremolite
> Amosite   } natural and leached
> Anthophyllite
> Crocidolite
> Zirconia E fiber (neodymia stabilized)
> TX fiber (nemolite:hydrated magnesia mineral)
> Potassium titanate fiber (PKT)
> Boron nitride fiber
> Silicon carbide fiber
> Ceria powder
> Titania powder

Several proprietary materials were also tested:

> ACCO-I (American Cyanamid Co)
> Ace-Sil (Amerace Corporation)
> Chrysotile-PKT-Neoprene bonded (Pratt & Whitney Aircraft)

The results of these tests, in terms of percentage weight loss of the specimen during the test, are given in Table 1. The conclusions derived from these tests are:

TABLE 1

Chemical Compatibility

Specimen Identification	Test Time(Hr)	Test Temp(°C)	KOH Conc.	% Wgt. Loss	Remarks
Chrysotile 1600	1000	150	30	19. 8	60-mil board
Chrysotile 1600	1000	150	40	30. 6	60-mil board
Chrysotile 1600	1000	150	50	59. 5	60-mil board
Chrysotile 2600	1000	150	40	25. 1	60-mil board
Chrysotile 2600	1000	150	50	38. 0	60-mil board
Chrysotile 2600	1000	150	60	38. 8	60-mil board
Chrysotile 3600	1000	150	50	37. 2	20-mil paper
Chrysotile 3600	1000	150	60	39. 9	20-mil paper
Chrysotile 3600	1000	150	30	7. 4	20-mil paper
Chrysotile 4600	1000	150	60	39. 5	20-mil paper
Chrysotile 4600	1000	150	30	19. 5	20-mil paper
Chrysotile 4600	1000	150	40	22. 5	20-mil paper
ACE-SIL	100	100	30	27. 9	
ACE-SIL	100	100	50	27. 7	
ACE-SIL	100	150	30	27. 7	
ACE-SIL	100	150	50	25. 3	
Potassium Titanate with Asbestos and Neoprene Binder	100	100	30	7. 2	
"	100	100	50	8. 4	
"	100	150	30	10. 7	
"	100	150	50	17. 1	
ACCO No. 1	100	100	30	3. 0	
ACCO No. 1	100	100	50	11. 2	
ACCO No. 1	100	150	30	19. 9	
ACCO No. 1	100	150	50	45. 5	
ACCO No. 1	1000	150	30	35. 4	
ACCO No. 1	1000	150	30	33. 2	
ACCO No. 1	1000	150	50	71. 0	
ACCO No. 1	1000	150	50	76. 9	

TABLE 1 (Continued)

Specimen Identification	Test Time(Hr)	Test Temp(°C)	KOH Conc.	% Wgt. Loss	Remarks
Boron Nitride	100	100	30	93.4	Totally dissolved
Boron Nitride	100	100	50	98.3	Totally dissolved
Boron Nitride	100	150	30	99.8	Totally dissolved
Boron Nitride	100	150	50	99.9	Totally dissolved
Boron Nitride	1000	150	30		Totally dissolved
Boron Nitride	1000	150	30		Totally dissolved
Boron Nitride	1000	150	50		Totally dissolved
Boron Nitride	1000	150	50		Totally dissolved
Potassium Titanate (Tipersul Pulp)	1000	150	30	2.7	
"	1000	150	30	8.6	
"	1000	150	50	13.4	
"	1000	150	50	7.2	
"	100	100	30	4.0	
"	100	100	50	8.2	
"	100	150	30	0.4	
"	100	150	50	0.6	
Zirconia E	1000	150	30	0.2	
Zirconia E	1000	150	30	0.3	
Zirconia E	1000	150	50	0.7	
Zirconia E	1000	150	50	0.6	
Zirconia E	100	100	30	0.1	
Zirconia E	100	100	50	0.1	
Zirconia E	100	150	30	0.4	
Zirconia E	100	150	50	0.3	
TX Fiber	1000	150	30	20.5	
TX Fiber	1000	150	50	3.6	
TX Fiber	1000	150	30	-	Lost sample
TX Fiber	1000	150	50	37.3	
TX Fiber	100	100	30	5.5	
TX Fiber	100	100	50	1.5	
TX Fiber	100	150	30	1.6	
TX Fiber	100	150	50	1.7	

TABLE 1 (Continued)

Specimen Identification	Test Time (Hr)	Test Temp (°C)	KOH Conc.	% Wgt. Loss	Remarks
Amosite	100	100	30	6.8	
Amosite	100	100	50	30.3	
Amosite	100	150	30	9.7	
Amosite	100	150	50	39.2	
Crocidolite	100	100	30	7.0	
Crocidolite	100	100	50	26.9	
Crocidolite	100	150	30	37.2	
Crocidolite	100	150	50	47.4	
Anthophyllite	100	100	30	3.0	
Anthophyllite	100	100	50	7.5	
Anthophyllite	100	150	30	9.0	
Anthophyllite	100	150	50	25.6	
Tremolite	100	100	30	4.6	
Tremolite	100	100	50	5.5	
Tremolite	100	150	30	7.5	
Tremolite	100	150	50	12.9	
Silicon Carbide (wool)	100	150	50	14.6	
Ceric Oxide	1000	150	30	1.9	
Ceric Oxide	1000	150	30	1.2	
Ceric Oxide	1000	150	50	0.6	
Ceric Oxide	1000	150	50	1.8	
Ceric Oxide	1000	100	30	1.5	
Ceric Oxide	1000	100	30	1.6	
Ceric Oxide	1000	100	50	1.8	
Ceric Oxide	1000	100	50	1.2	
Potassium Titanate PKT	1000	100	30	4.1	
Potassium Titanate PKT	1000	100	50	3.0	

TABLE 1 (Continued)

Compatibility Test (Weight Gain)

Specimen Identification	Test Time (Hr)	Test Temp (°C)	KOH Conc.	% Wgt. Gain	Remarks
Potassium Titanate PKT	1000	150	30	8.4	
Potassium Titanate PKT	1000	150	30	-	No loss or gain
Potassium Titanate PKT	1000	150	50	32.7	
Potassium Titanate PKT	1000	150	50	-	Lost sample
Potassium Titanate PKT	1000	100	30	9.8	
Potassium Titanate PKT	1000	100	50	5.8	
Titanium Oxide	1000	150	30	34.3	
Titanium Oxide	1000	150	30	30.4	
Titanium Oxide	1000	150	50	60.4	Both had a thin
Titanium Oxide	1000	150	50	87.7	film of transparent material present
Titanium Oxide	1000	100	30	6.8	
Titanium Oxide	1000	100	30	6.3	
Titanium Oxide	1000	100	50	41.3	
Titanium Oxide	1000	100	50	44.8	

1.   The asbestoses, being silicates, are inherently reactive with KOH and are, therefore, unsuitable. Pretreatment of the asbestos with dilute acid or sequestering agent removes the metallic cations from the fiber, leaving silica, which is readily soluble in alkali.

2.   TX fiber is superior in resistance to KOH, but its high iron content renders it unsuitable for matrix service.

3.   The three proprietary mats are poor.

4.   Boron nitride dissolves completely, and silicon carbide fiber is poor.

5.   Zirconia E fiber and ceria powder are virtually unchanged.

6.   PKT and titania change only slightly during the 100 hour test, but both gain weight significantly during the 1000 hours*. The titania developed an insoluble, gelatinous film, which may be a hydrated titania, but we have not established a chemical identification.

The four materials selected for further study on the basis of the initial chemical degradation tests are Zirconia E, PKT fiber, ceria, and titania. The remaining chemical degradation tests - notably at 200°C - are still in progress.

These four selected materials were subjected to the remaining test program which included a more intensive look at the as-received materials as well as the fabrication and evaluation of mats of these materials.

---

* This information about the weight gain of titania and PKT was obtained at the end of the 1000-hour chemical compatibility tests, actually after the program of tests with mats of these materials had been completed. With this new evidence that PKT and titania, while remaining insoluble, undergo changes due probably to hydration, questions arise concerning the matrix properties of these changed materials. It is conceivable that with the development of new particle surface properties, the bubble pressure may be greatly improved and the electrolytic resistance may increase. The particles may also develop a coherence that will obviate the need for the added fibrous binder that was used in mats made for this program.

VI   EVALUATION OF SELECTED MATERIALS

The four materials (zirconia fiber, PKT, ceria and titania) selected in the chemical compatibility tests were evaluated by the full complement of tests in this part of the program.   This included a further study of the as-received fibers or powders, the preparation of 20-mil and 60-mil thick mats from these materials, the study of the dry mats, and an evaluation of the mats when wet with KOH. For the preparation of mats from these materials, 10% chrysotile fiber was added to the base constituent to help improve the structural integrity of the mats.

Starting Materials

Chemical composition. - The chemical composition of the chrysotile asbestos and the other four materials used in mat preparation are listed below.   These analyses have been supplied by the vendors of the respective materials.

Fuel Cell Asbestos (Arizona chrysotile from Johns Manville)

The composition included in the Task 1 report is repeated here:

SiO_2	41. 86%	42. 14%
MgO	42. 78	42. 80
CaO	2. 19	1. 70
Fe_2O_3	0. 85	0. 87

PKT (Pigmentary Potassium Titanate from duPont)

TiO_2	85%
K_2O	11
K_2SO_4	3. 0
KCl	0. 1
Fe	100 ppm

Titania (TiO_2) (Fisher Scientific Co. , Certified Anhydrous)

Water soluble salts	0. 05%
Arsenic (As)	0. 00024
Iron (Fe)	0. 01
Lead (Pb)	0. 002
Zinc (Z)	0. 01

Zirconia Fiber (H. I. Thomas Fiberglass Co.)

This material is basically zirconium oxide, stabilized by 10-15% neodymia. Semiquantitative spectrographic analysis by a commercial laboratory yielded the following results:

Zirconium	73%
Hafnium	0.74
Magnesium	0.012
Titanium	0.068
Silicon	0.13
Calcium	0.003

Ceria (Ceric oxide - Fisher Scientific Co. Certified Grade)

CeO_2	99.5% min.
Di_2O_3	0.05 max.
Fe_2O_3	0.003
P_2O_5	0.005

Our spectrographic analysis revealed appreciable calcium, but no quantitative estimate was attempted.

Fiber structure. - The natural asbestoses - amosite, anthophyllite, tremolite, and crocidolite - and TX fiber were photographed at 10X magnification (Figures 3, 4, 5, 6, and 7). Although these materials were not selected for the comprehensive testing program, the photographs reveal the wide difference in character of the material. The fiber length and degree of fiber separation are largely determined by the processing each one has received, but some inherent differences are evident. Tremolite is a very soft, "ropey" fiber, while TX fiber is fine, loose, and tends to be brittle. The anthophyllite fibers are short and poorly resolved.

The Zirconia E fiber is evidently a smooth surfaced fiber, tends to curl, but the fibers tend to remain separated (Figure 8). The potassium titanate (PKT) is a short straight fiber that tends strongly to clump together (Figure 9 and 10). The ceria and titania are not included here since they were purchased as powders and, therefore, have no fibrous structure.
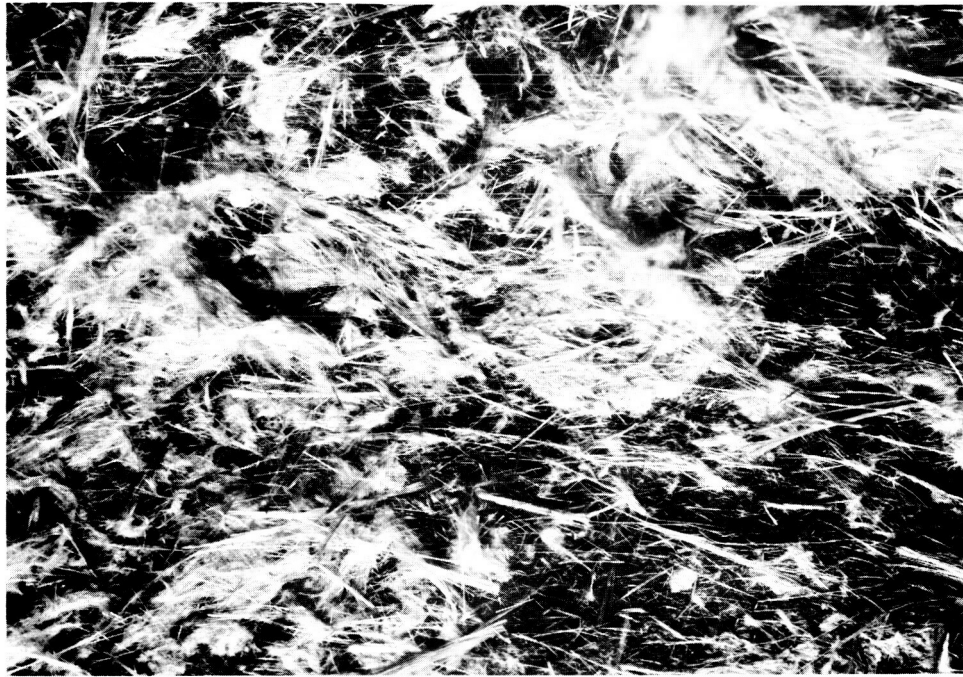
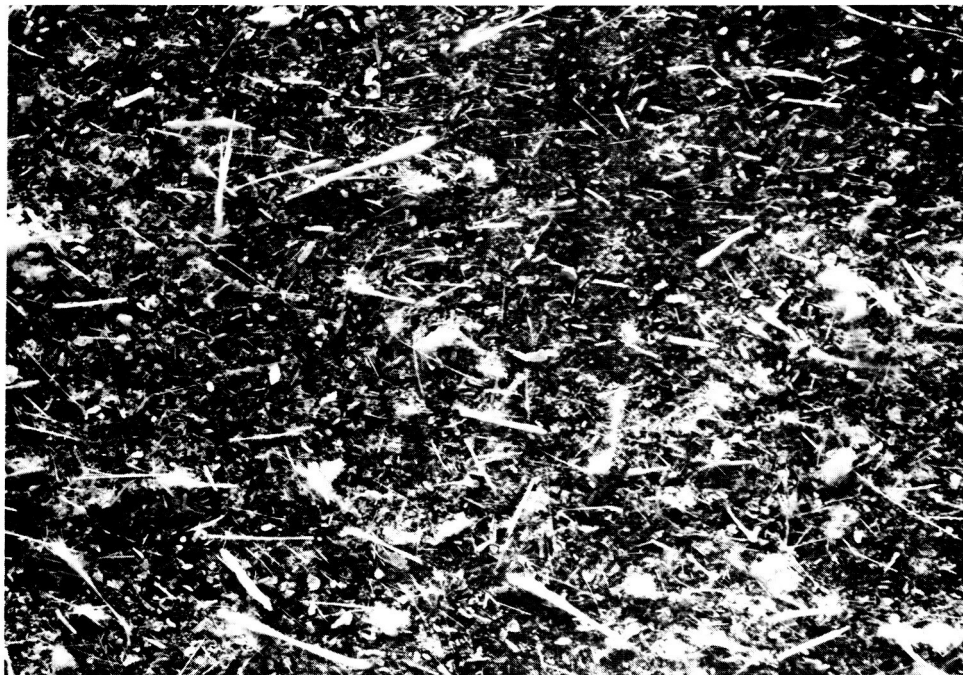Figure 3.　　Amosite (10X)

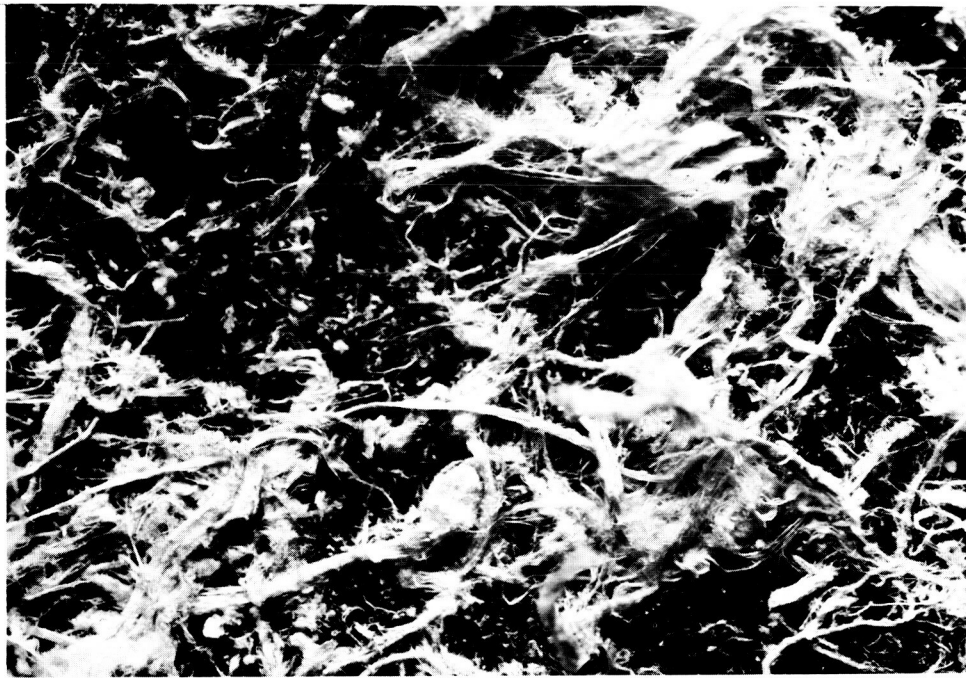Figure 4.　　Anthophyllite (10X)

Figure 5.   Tremolite (10X)

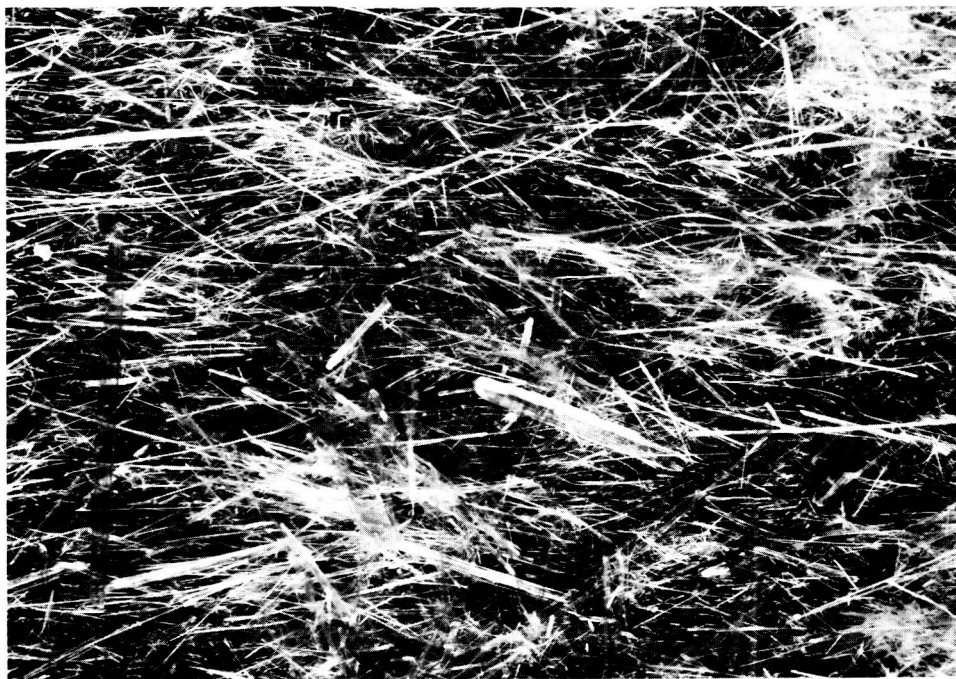Figure 6.   Crocidolite (10X)

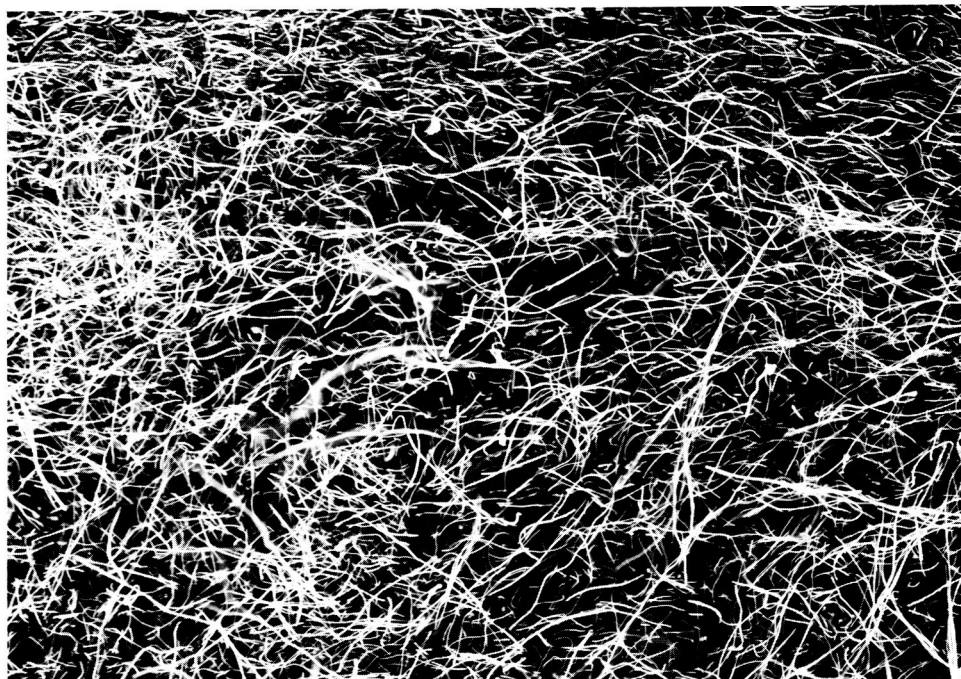Figure 7.   TX Fiber (10X)

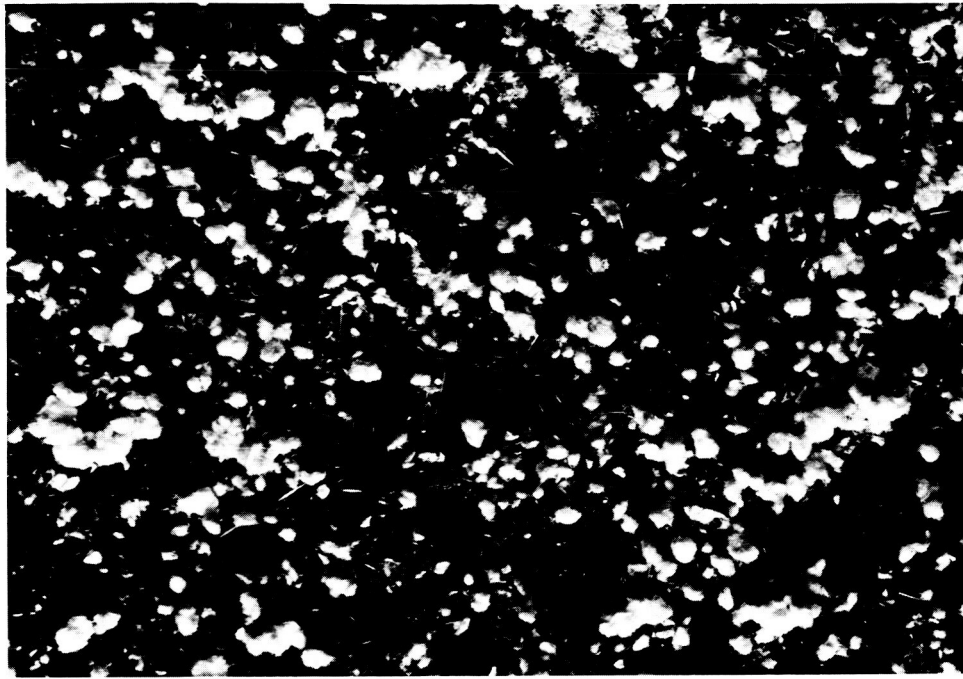Figure 8.   Zirconia E Fiber (10X)

Figure 9.   Potassium Titanate PKT (10X)

Figure 10.   Potassium Titanate PKT (10,000X)

Surface area. - Surface areas of the component materials selected for incorporation in mats were measured by the nitrogen adsorption technique, with the Perkin Elmer Sorptometer, Model 212B.

Ceria	2. 08 m^2/g
Chrysotile	50 m^2/g
Potassium Titanate	10. 2 m^2/g
Titanium Oxide	8. 16 m^2/g
Zirconia E	2. 85 m^2/g

The manufacturer, H. I. Thompson Fiberglass Co, reports the value of 100m^2/g for Zirconia E fiber. A look at the macrograph of this fiber (Figure 8), however, would indicate that our experimental value of 2. 85 m^2/g is closer to what would be expected for this size of fiber.

Preparation of Mats

Because mats composed individually of the four selected materials - PKT, ceria, zirconia, and titania - are too weak and brittle to be tested, these materials were blended with 10 weight percent of chrysotile asbestos fibers to add structural integrity to the mats. The components for each mat were weighed separately and then blended together in water by prolonged gentle mechanical stirring.

Chrysotile fiber, when well dispersed, forms a very slowly settling aqueous suspension. Mats are best prepared with a sheet mold which consists essentially of a reservoir equipped with a fine screen bottom and a water-column drain to generate about 30 inches of hydrostatic pressure at the screen. The dilute suspension of fiber is poured into the reservoir, agitated, allowed to become quiescent, and then quickly sucked down against the screen. The mat is then lifted off the screen, pressed between absorbent paper, and dried.

A sheet mold was built in this laboratory to make mats of chrysotile and similar fibers (Figure 11). The reservoir was made unusually tall to contain, in one filling, the quantity of dilute suspension needed for a 60-mil thick mat. The screen was replaced by a layer of 1-inch thick, fine-pore polyurethane sponge on a perforated Plexiglass plate support. The sponge was an effective non-clogging filter bed, from which the mat could be cleanly separated. The wet mat was then sandwiched between layers of absorbent paper and plastic plates and compressed by rolling with a 20 lb. steel cylinder, after which it was dried in a laboratory oven.
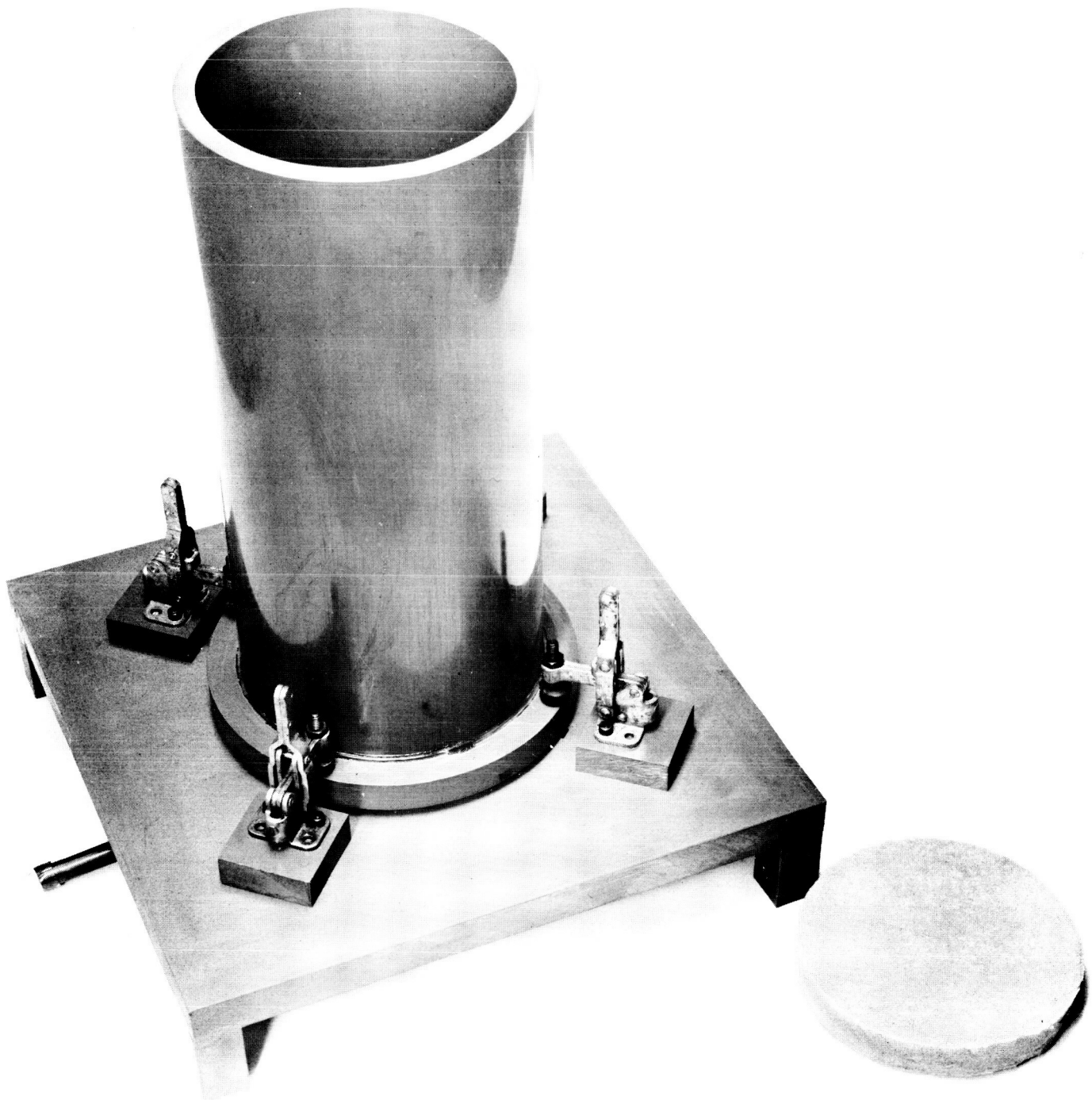
Figure 11.   Mat Casting Apparatus.

The sheet mold cannot be used with the other selected materials. In contrast with chrysotile fiber, the other materials are more dense and settle much faster from a dilute suspension. When mixed with chrysotile in dilute suspension, the great disparity in settling rates causes gross stratification in the mat that is formed. In order to preserve the desired homogeneity in the mat, the suspension must be made quite concentrated and it must be cast quickly. The polyurethane sponge, which served so well as a bed for the casting of fibrous chrysotile, is unable to retain the small-particle powders. Consequently, we used a standard laboratory Buchner funnel with filter paper for preparation of the composite mats. After being formed in the funnel, the mat was placed on paper towels to remove most of the water by capillarity. Finally, it was placed between paper towels, and compressed in a small manual hydraulic press.

Composites with zirconia fiber were completely crushed by the hydraulic pressing, and therefore required more gentle treatment. We compacted the zirconia composite mats by placing them between layers of absorbent paper sandwiched between lucite plates (with metal shims to establish the final mat thickness) and rolling manually with a 20-lb. steel cylinder.

The mats prepared for testing were to be of two thicknesses: 0.020 ±0.002 inch and 0.060 ± 0.004 inch. The mats containing PKT, ceria, and titania were made conforming to the thickness requirements by maintaining a constant molding technique and final compaction pressure, and by controlling the weight of material in a mat. In the case of the zirconia fiber composites, the weight of material per mat was adjusted to permit the final compaction without incurring undue destruction of the brittle fibers. In all cases, the mats of each composition produced for test were uniform in thickness and weight.

Dry Mat Properties

Strength. - Tensile tests were performed on the Instron Tensile Tester. The specimens were die-cut rectangles, 2 x 3 inches, mounted to provide a gage length of 1 inch. Cross-head was 0.50 inch per minute.

Typical extension curves are presented in Figure 12, and the tensile strength results are recorded in Table 2. It is noted that these mats are approximately only 10-15% as strong as the Fuel Cell Asbestos mats. It is likely, therefore, that most of the strength of these mats can be attributed to the 10% chrysotile fibers added to the mat.

B 961 B

LOAD (POUNDS)

0

1

2

3

ELONGATION (INCHES)

.05

.10

.15

A

B

C

D

A   TITANIUM OXIDE - CHRYSOTILE

B   CERIC OXIDE - CHRYSOTILE

C   ZIRCONIA E - CHRYSOTILE

D   POTASSIUM TITANATE PKT - CHRYSOTILE
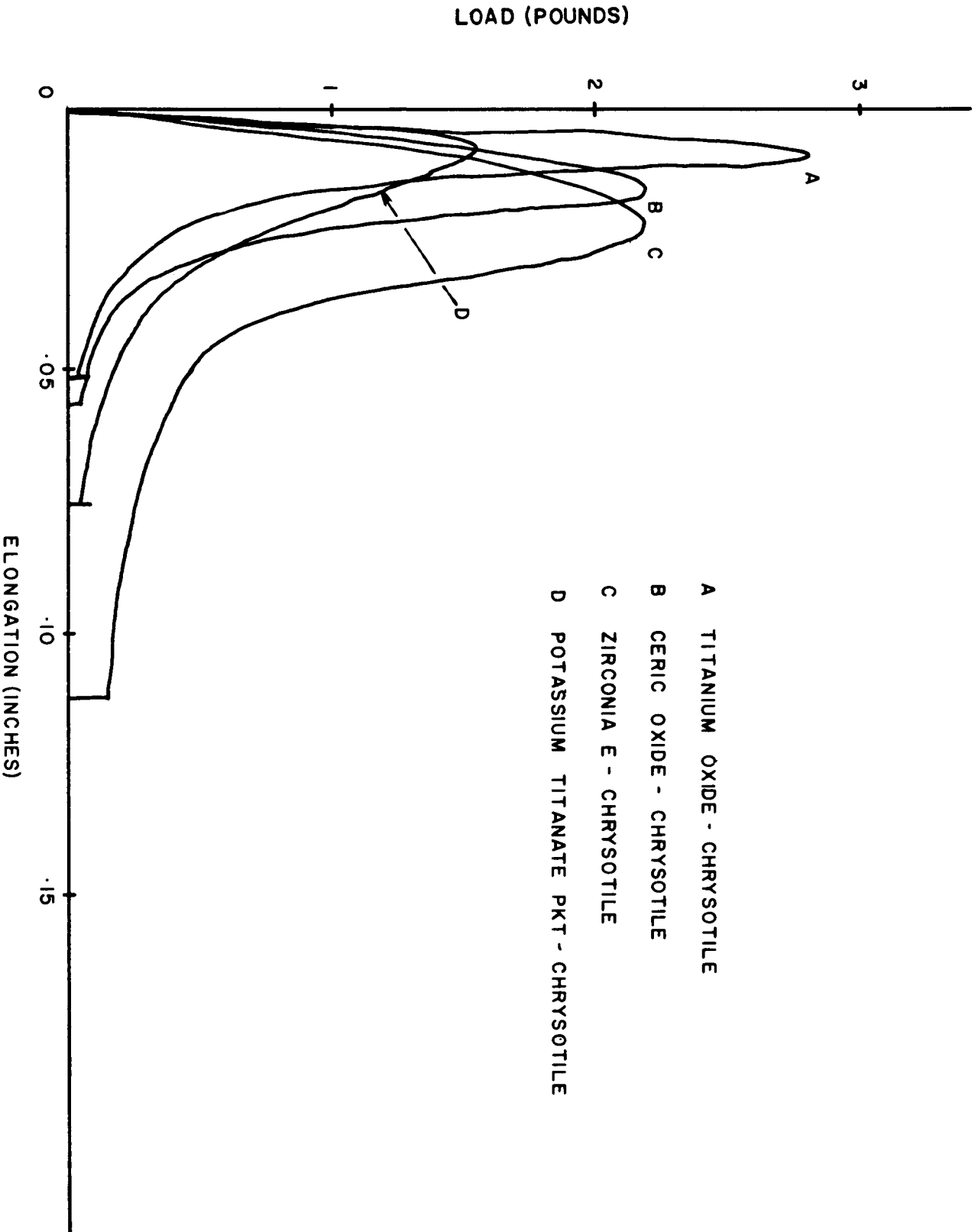
Figure 12.   Tensile Curves.

TABLE 2

Tensile Tests

Specimen	Thickness	Load(lbs)*	Tensile Strength(psi)
Ceric Oxide-Chrysotile	.020"	.715	17.9
Ceric Oxide-Chrysotile	.020"	.895	22.4
Ceric Oxide-Chrysotile	.060"	4.06	33.8
Ceric Oxide-Chrysotile	.060"	2.295	19.2
Titanium Oxide-Chrysotile	.020"	.71	17.7
Titanium Oxide-Chrysotile	.020"	.54	13.5
Titanium Oxide-Chrysotile	.060"	3.18	25.6
Titanium Oxide-Chrysotile	.060"	2.89	24.1
Potassium Titanate PKT -Chrysotile	.020"	.550	13.7
Potassium Titanate PKT -Chrysotile	.020"	.505	12.6
Potassium Titanate PKT -Chrysotile	.060"	1.955	16.3
Potassium Titanate PKT -Chrysotile	.060"	1.615	13.5
Zirconia E-Chrysotile	.020"	.620	15.5
Zirconia E-Chrysotile	.020"	.725	18.1
Zirconia E-Chrysotile	.060"	2.305	19.3
Zirconia E-Chrysotile	.060"	2.20	18.4
Fuel Cell Asbestos**	.020"		150
Fuel Cell Asbestos**	.060"		80-170

* Load on a 2" wide cross-section of the listed mat thickness
**Results from Task 1 of the program

Density. - True densities were measured with the Beckmann Air Comparison Pycnometer. Values for the mat components separately are:

Ceria	6.93 g/cc
Chrysotile	2.73 g/cc
Potassium Titanate (PKT)	3.32 g/cc
Titania	4.03 g/cc
Zirconia E	4.70 g/cc

True densities of the finished mats were also determined, the results are recorded in Table 3. The mat porosity was also computed from a comparison of true density with the geometric density. Porosity in the 70-85% range was obtained in these mats. This appears favorable compared to the 70% porosity typical of the standard asbestos mats.

Thickness variations. - Thickness was measured with a dial gage instrument equipped with a 1/2-inch diameter foot and dead-weight loaded to 5 lb per square inch. Only those mats were retained for testing which fulfilled the thickness tolerance requirements, namely ±0.002 inch for the 0.020-inch mats and ±0.004 inch for the 0.060-inch mats.

Pore size distribution. - The pore size distribution of these mats was measured by the mercury intrusion method using an Aminco-Winslow Porosimeter. The resultant pore spectra curves are shown in Figure 13. These results show that the titania and the PKT mats contain pores mostly in the sub-micron range. The ceria mat has most of its pores in the 1-1.5 micron range, and the zirconia mat contains pores mostly in the 10-micron range. As will be seen later, this relatively large pore size of the zirconia mat results in poor gas-sealing behavior compared to the other mats.

Mercury intrusion curves could not be obtained on the new Fuel Cell Grade Asbestos mats studied in Task 1 because their flexibility caused them to collapse under the mercury pressure. However, some prior data (obtained by mercury intrusion on used asbestos that had become stiff after removal from an operating cell) indicated that Fuel Cell Grade Asbestos has an average pore size in the one-half micron range. This is close to the pore size of the titania and the PKT mats made for this program. This indicates that these mats should have a capability for demonstrating good gas sealing properties if they can retain their structure when wet with electrolyte.

TABLE 3

Density of Mats

Specimen Identification	Actual Density	Apparent Density	% Void Volume
Ceric Oxide-Chrysotile			
.020" Thickness	6.24g/cc	1.64g/cc	74
.060" Thickness	6.18g/cc	1.80g/cc	71
Zirconia E-Chrysotile			
.020" Thickness	4.97g/cc	0.67g/cc	86
.060" Thickness	5.39g/cc	0.72g/cc	87
Potassium Titanate PKT-Chrysotile			
.060" Thickness	3.59g/cc	0.47g/cc	87
Titanium Oxide-Chrysotile			
.020" Thickness	3.67g/cc	0.98g/cc	73
.060" Thickness	3.85g/cc	1.16g/cc	70

PENETRATION CC

PORE DIAMETER MICRONS

A   POTASSIUM TITANATE PKT - CHRYSOTILE

B   TITANIUM OXIDE - CHRYSOTILE

C   CERIC OXIDE - CHRYSOTILE

D   ZIRCONIA E - CHRYSOTILE
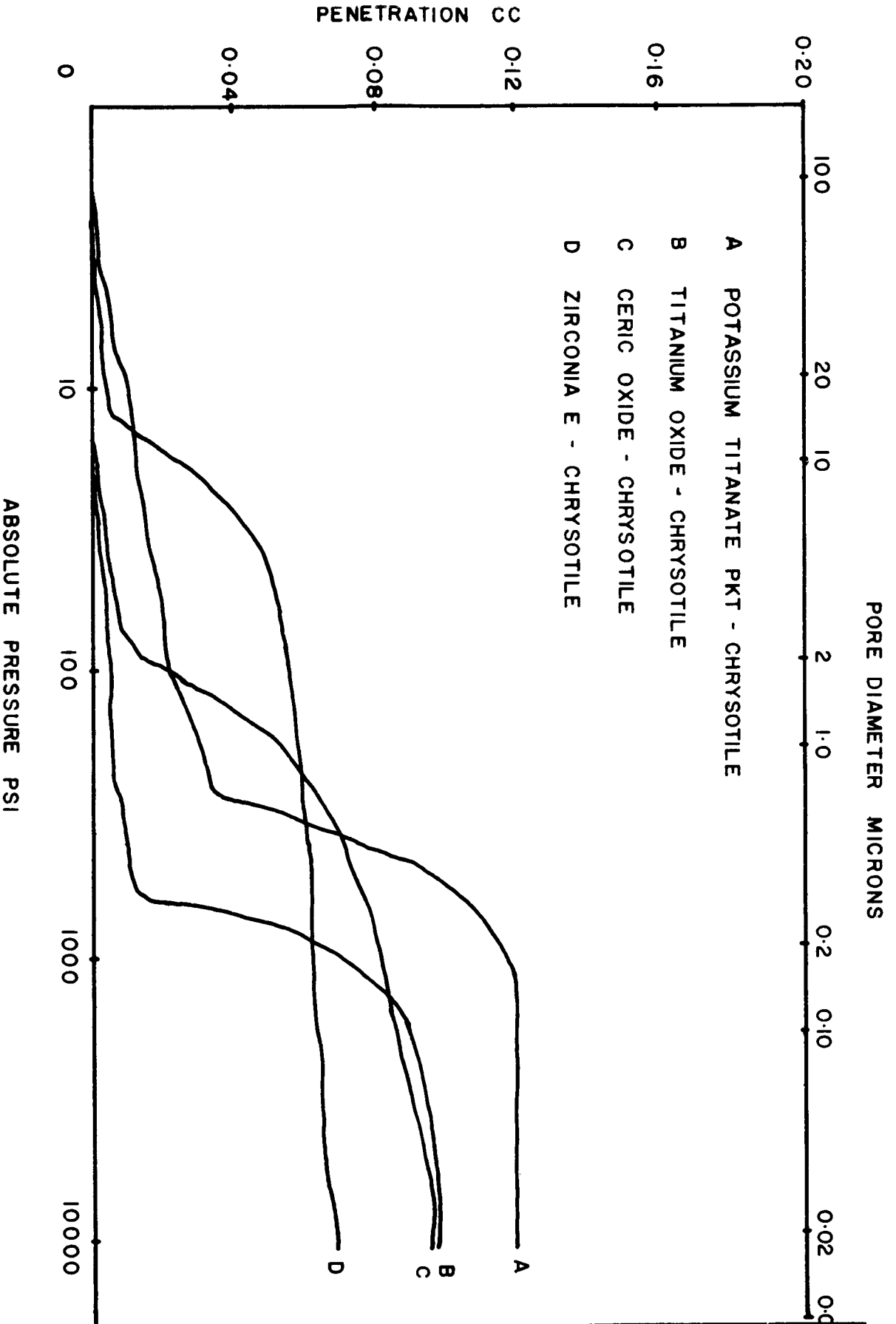
ABSOLUTE PRESSURE PSI

Figure 13.   Pore size distribution of dry mats of the various materials evaluated for cell separators.

Electrolyte Absorption and Retention

  The technique used for this test was essentially that described in the Task I Summary Report of this program, except that in the recent tests all the manipulations - weighing, saturating centrifuging, etc. - have been performed without transferring the specimen from its supporting screen. The mats, when saturated with KOH electrolyte, are too fragile to permit such a transfer. The results from these tests are summarized in Table 4.

  As a basis on which to compare these results, it is recalled that the 20-mil asbestos absorbed 3.8 times its weight in KOH, and the 60-mil mat absorbed 5.6 times its weight. On this basis, the zirconia mat and the PKT mat compare favorably with the standard asbestos in ability to absorb electrolyte. The mats made from the powders (ceria and titania) do not compare as favorably with the asbestos. Part of this difference is due to the higher density of the powders compared with the chrysotile asbestos. If this density difference is corrected for, however, these mats still have only about one half the absorbancy of asbestos on a volume-to-volume basis.

  The ability of the mats to retain electrolyte under the action of an acceleration force of 25g compares well with the asbestos mats. The mats made from the zirconia fiber lose significantly more than the others. However, the ability of the 60-mil zirconia mat to retain 78% of the electrolyte during the test is about the same as was experienced with the 60-mil asbestos mats.

Electrolytic Resistance

  The measurements of electrolytic resistance of chrysotile paper and millboard were performed with a two-piece cell (Figure 14) of the design described by J. E. Cooper and A. Fleischer (Characteristics of Separators for Alkaline Silver Oxide-Zinc Secondary Batteries, Screening Method). In place of the Hg-HgO reference electrodes specified by these authors, we substituted dynamic hydrogen electrodes. Generally there is a small potential difference between the two hydrogen electrodes, but this causes no difficulty.

  The test of a specimen consists in measuring the potential difference between the two hydrogen electrodes with and without current through the specimen. The net change in potential is a measure of the IR drop across the specimen.

TABLE 4

Electrolyte Absorption and Retention Under 25G Acceleration

Specimen	Thick. Inches	Weight of Spec, gm	Wgt of Absorb. Solution, gm	Weight Ratio Absorbed	Weight of Retained Soln, gm	Weight Ratio Retained	% Retained
Ceric Oxide-Chrysotile	.020	.4090	.4884	1.19	.4755	1.16	
Ceric Oxide-Chrysotile	.020	.3856	.5671	1.47	.5218	1.35	
			Average	1.33	Average	1.26	95
Ceric Oxide-Chrysotile	.060	1.5494	1.6199	1.04	1.4770	.95	
Ceric Oxide-Chrysotile	.060	1.3713	1.4249	1.04	1.3153	.96	
			Average	1.04	Average	.96	92
Titanium Oxide-Chrysotile	.020	.2351	.4189	1.78	.4088	1.74	
Titanium Oxide-Chrysotile	.020	.2215	.4172	1.88	.4055	1.83	
			Average	1.83	Average	1.78	97
Titanium Oxide-Chrysotile	.060	.7374	1.0564	1.43	1.0439	1.42	
Titanium Oxide-Chrysotile	.060	.7589	1.0930	1.44	1.0809	1.42	
			Average	1.44	Average	1.42	98
Zirconia E-Chrysotile	.020	.1273	.7966	6.26	.6295	4.94	
Zirconia E-Chrysotile	.020	.1702	.8589	5.05	.6525	3.88	
			Average	5.66	Average	4.38	77
Zirconia E-Chrysotile	.060	.4871	1.6911	3.47	1.3520	2.78	
Zirconia E-Chrysotile	.060	.4802	1.6374	3.41	1.2513	2.60	
			Average	3.44	Average	2.69	78
Potassium Titanate PKT-Chrysotile	.020	.0941	.6201	6.59	.5367	5.70	
Potassium Titanate PKT-Chrysotile	.020	.1029	.6639	6.45	.6171	6.00	
			Average	6.52	Average	5.85	90
Potassium Titanate PKT-Chrysotile	.060	.3546	1.6558	4.67	1.6310	4.60	
Potassium Titanate PKT-Chrysotile	.060	.3494	1.6310	4.67	1.5856	4.54	
			Average	4.67	Average	4.57	98

Figure 14. Electrolytic Resistance Cell.

SPECIMEN

1/8" PLEXIGLAS SPACER
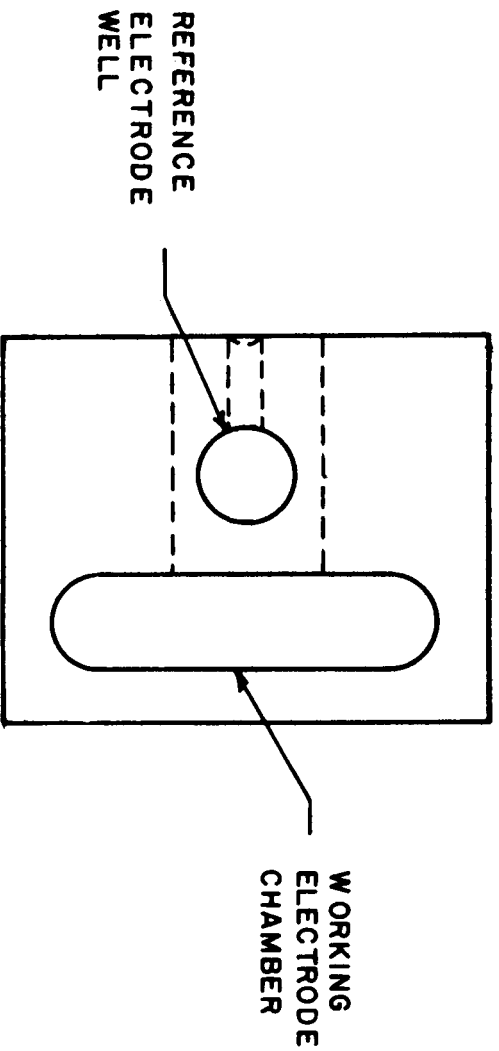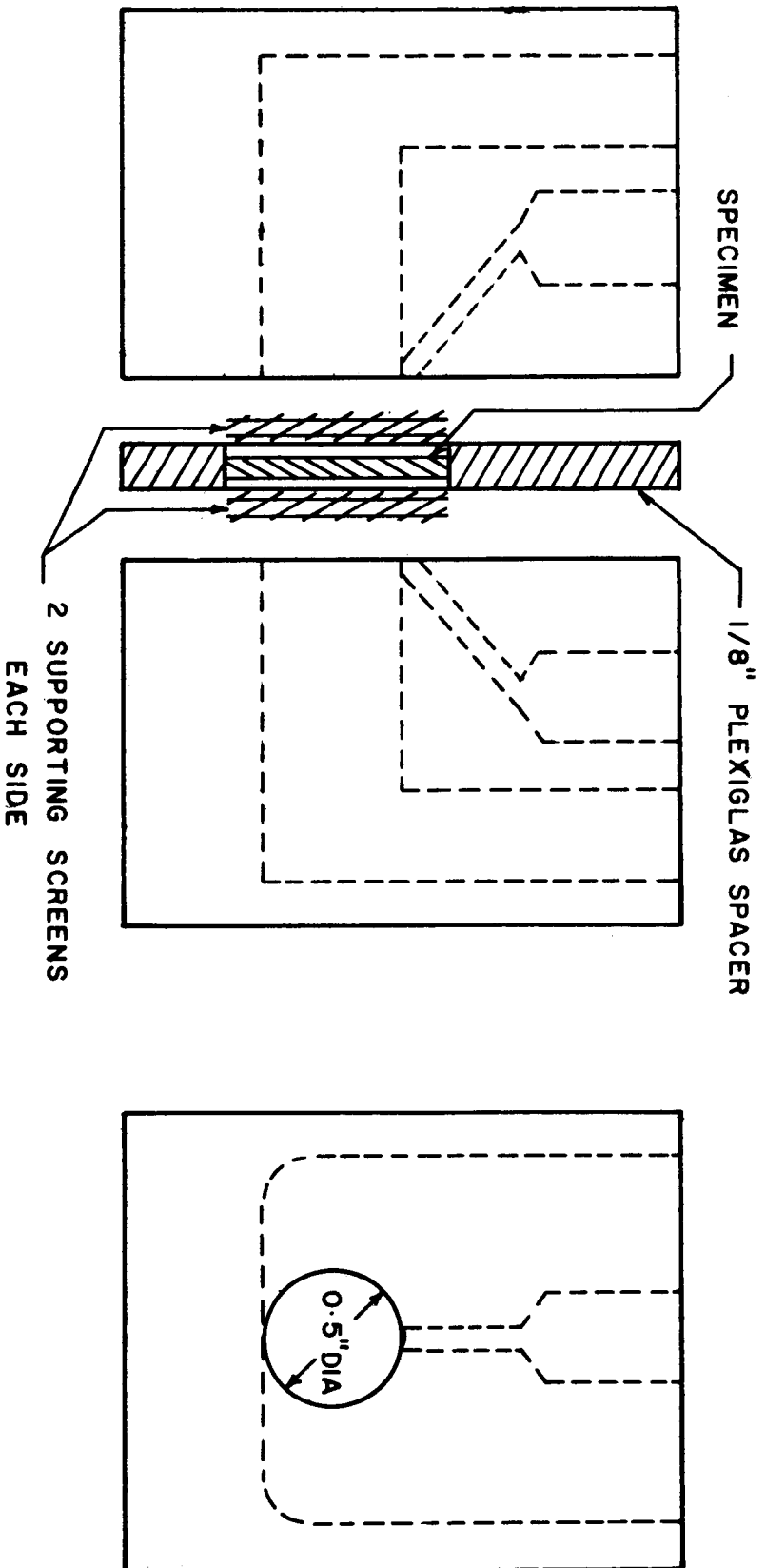
2 SUPPORTING SCREENS
EACH SIDE

REFERENCE
ELECTRODE
WELL

WORKING
ELECTRODE
CHAMBER

0.5" DIA

When the chrysotile matrices were tested, the specimens were simply clamped between the cell halves and permitted to expand freely. However, the matrices prepared in Task 2 disintegrate when saturated with electrolyte, and consequently, a physical support was required for this test. The cell was modified by installing between the cell halves a Plexiglass sheet (1/8 inch thick) with a 5/8 inch hole bored coaxial with the 1/2" diameter hole that forms the electrolyte channel. This arrangment provides a chamber in which the specimen can be mounted between double layers of supporting metal screen. Under these conditions, the specimen can attain a maximum thickness of about 60 mils.

By measuring the attenuation of light to a photographic photometer, a single layer of metal screen was estimated to be about 50% transmitting.

A question of data interpretation arises. The exposed diameter of the specimen is now 5/8 inch rather than 1/2 inch. This constitutes an area increase of 56%. However, this increased area is a rim 1/16 wide lying outside the region of rectilinear electrical flow lines. The degree to which this rim area contributes to the total specimen conductivity is not known. Also, the degree to which the supporting screens reduce the effective specimen area is not known. A test was therefore performed to provide a factor of relationship between the total geometric area and the effective conducting area of the supported specimen.

For this test we selected Ace-Sil, a well-bonded non-swelling microporous rubber separator material of 27-mil thickness. A piece of this material was first tested without, and then with, the Plexiglass separator and supporting screens. First, the specimen was mounted directly between the test-cell halves so that a 1/2 inch diameter disk of surface was fully exposed to the electrolyte. Data from this test yielded the true electrolytic resistance of the specimen.

In the second test, the specimen, trimmed to 5/8" diameter, was mounted between the double layers of supporting screen in the Plexiglass recess between the test cell halves. The results of this test indicated just about four times the resistance of the unsupported specimen.

Accordingly, in the data reported for electrolytic resistance (Table 5), the computations are based on the full specimen area (1.98 cm^2) and the final value of resistance is reduced by the factor of four. In order to establish a basis of relationship, specimens of chrysotile were also measured and the data is included in Table 5.

TABLE 5

Electrolytic Resistance of Mats

(Current 87 ma, Specimen Area 1.98 cm^2)

Specimen	Thickness (inches)	R of Mat* (ohm-cm^2)	Specific Resistances (ohm-cm)
Potassium Titanate (PKT)	0.020	0.209	4.13
	0.020	0.218	4.30
Zirconia E	0.020	0.198	3.90
	0.020	0.181	3.58
	0.020	0.180	3.55
	0.060	0.228	1.50
	0.060	0.226	1.49
	0.060	0.226	1.49
Titanium Oxide	0.020	0.170	3.36
	0.020	0.176	3.47
	0.060	0.285	1.87
	0.060	0.260	1.71
Ceric Oxide	0.020	0.213	4.20
	0.020	0.202	3.98
	0.060	0.319	2.10
	0.060	0.306	2.01
Fuel Cell Asbestos	0.020	0.24	4.74**
	0.060	0.36	2.37**

* These derived values of resistance incorporate the assumption that all specimens swell to fill completely the 0.060-inch thick space between the supporting screens and, therefore, replace a 0.060-inch thick layer of KOH solution. This may account for the general difference between computed values for the 0.020-inch and 0.060-inch thick mats.

**These values compare with values of 9 ohm-cm for the 20-mil paper and 5.5 ohm-cm for the 60-mil mat determined during Task 1 of the program on the unmodified test apparatus.

Incidentally, inasmuch as the supporting screens are used in pairs on each side of the specimen, the question arose, whether the orientation of the contiguous screens influences the effective conducting area. Tests were, therefore, performed using the Ace-Sil membrane with the screens oriented wires-parallel and wires-crossed 45°. The data were practically identical, and we conclude that screen orientation is not critical.

The data listed in Table 5 show several significant things. First, the resistance of the Fuel Cell Asbestos as measured by this modified test rig was about one-half of that determined by the original test rig in Task 1 of the program. This probably can be attributed to the restricted degree of swelling that can take place in the modified test rig.

The second observation is the encouraging fact that all the mats tested in this part of the program showed less resistance to ionic conduction than the Fuel Cell Grade Asbestos mats. This indicates that these materials may offer real promise in the development of improved cell separators.

Gas Permeability

The gas that permeates the specimen under a pressure differential is measured by a water bubbler. As expected, all the dry mats are permeable (Table 6). The ratio of pressure differential to flow ratio in terms of bubbles per second was calculated for each test. This ratio reveals a satisfactory consistency of the data for the potassium titanate, the titania, and the ceria mats. In each case, the thin mats are more permeable than the thick ones, and in the case of the powders (titania and ceria) the permeabilities are related inversely as the mat thicknesses. The more loosely-packed zirconia fiber mats reveal very little consistency of the test data.

Gas permeability data for the wet mats are recorded in Table 7. The net pressure recorded for each specimen is the pressure (with gradual increase) at which gas leakage was first detected. The ceria, titania, and the PKT mats demonstrated good gas sealing characteristics (particularly in the 60-mil mats) when they contain electrolyte in the 1 : 1 weight ratio. At higher electrolyte loadings, these mats leak gas because of loss of structural integrity.

TABLE 6

Gas Permeability of Dry Mat

Specimen	Thick. (inch)	Net Pressure (psi)	Flow Rate (Bubble/sec)	Ratio Flow Rate $\overline{\text{psi}}$
Zirconia E-Chrysotile	.060	.09	1.4	15.6
Zirconia E-Chrysotile	.060	.11	4.0	36.4
Zirconia E-Chrysotile	.060	.11	2.0	18.2
Zirconia E-Chrysotile	.060	.13	4.0	15.4
Zirconia E-Chrysotile	.060	.08	2.0	25.0
Zirconia E-Chrysotile	.060	.09	4.0	44.4
Zirconia E-Chrysotile	.020	.05	1.5	30.0
Zirconia E-Chrysotile	.020	.06	4.0	66.7
Zirconia E-Chrysotile	.020	.05	2.0	40.0
Zirconia E-Chrysotile	.020	.06	4.0	66.7
Zirconia E-Chrysotile	.020	.06	1.8	30.0
Zirconia E-Chrysotile	.020	.06	4.0	66.7
Potassium Titanate PKT-Chrysotile	.020	.07	3.0	41.6
Potassium Titanate PKT-Chrysotile	.020	.07	-	-
Potassium Titanate PKT-Chrysotile	.020	.07	3.0	41.6
Potassium Titanate PKT-Chrysotile	.060	.07	1.8	25..0
Potassium Titanate PKT-Chrysotile	.060	.07	1.6	22.2
Potassium Titanate PKT-Chrysotile	.060	.07	1.6	22.2
Titanium Oxide-Chrysotile	.060	.32	1.5	4.6
Titanium Oxide-Chrysotile	.060	.32	1.4	4.3
Titanium Oxide-Chrysotile	.020	.22	3.0	13.9
Titanium Oxide-Chrysotile	.020	.22	2.7	12.5
Ceric Oxide-Chrysotile	.060	.22	2.0	9.3
Ceric Oxide-Chrysotile	.060	.22	1.9	9.3
Ceric Oxide-Chrysotile	.020	.11	3.0	27.9
Ceric Oxide-Chrysotile	.020	.11	3.0	27.9

TABLE 7

Gas Permeability of Wet Mat

Specimen	Thick. (inch)	Electrolyte Ratio	Net* Pressure (psi)	Flow Rate (Bubble/sec)
Ceric Oxide-Chrysotile	.060	1 : 1	12.2	2.0
" " "	.060	1 : 1	12.2	.6
" " "	.020	1 : 1	0	Ruptured
" " "	.020	1 : 1	12.2	4.0
Titanium Oxide-Chrysotile	.060	1 : 1	12.2	3.0
" " "	.060	1 : 1	9.3	4.0
" " "	.020	1 : 1	0	Ruptured
" " "	.020	1 : 1	1.9	3.0
Potassium Titanate PKT-Chrysotile	.060	1 : 1	6.1	2.4
" " " "	.060	1 : 1	6.9	3.0
" " " "	.060	1 : 1	11.5	2.3
" " " "	.020	1 : 1	0.1	3.0
" " " "	.020	1 : 1	0.3	Ruptured
" " " "	.020	1 : 1	0.6	1.8
Zirconia E- Chrysotile	.060	1 : 1	1.5	First leakage
" "	.060	2 : 1	2.2	First leakage
" "	.060	3 : 1	0	Ruptured
" "	.060	1 : 1	1.2	First leakage
" "	.060	2 : 1	1.9	First leakage
" "	.060	3 : 1	2.0	First leakage
" "	.060	4 : 1	0	Ruptured
" "	.060	1 : 1	0.4	First leakage
" "	.060	2 : 1	1.4	First leakage
" "	.060	3 : 1	0	Ruptured
" "	.020	1 : 1	0.4	First leakage
" "	.020	1 : 1	0.4	First leakage
" "	.020	1 : 1	0.3	First leakage

* This is the pressure at which bubbling first occurred, so it may be considered the "bubble pressure" of the specimen.

The zirconia-fiber mats generally did not have as high a bubble pressure as the others. However, they were able to hold more electrolyte and still retain their structural integrity, so that the best gas sealing properties were obtained at electrolyte loadings generally greater than the 1:1 ratio.

Although the gas sealing properties of these mats may be ample for cell application, they are generally inferior to fuel cell asbestos in this attribute.

Liquid Permeability

Liquid permeabilities were measured by allowing water, under the pressure of a vertical column, to flow through the supported specimen. The average head of water pressure was 119.4 cm and the volume of water passed in a test was 1.12 ml. The results of these tests are shown in Table 8. Generally, these mats are considerably more permeable to liquid flow than the Fuel Cell Asbestos mats tested in Task 1.

In a general way, these data correlate with the gas permeabilities of the dry mats (Table 6). That is, the mat compositions that are the most permeable to gas also are the most permeable to liquid flow as indicated by short flow times in the liquid permeability tests. These data also have some correlation to the electrolytic resistance tests (Table 5) in that the asbestos has the highest resistance to both the liquid flow and electrolytic current flow, and the zirconia mats show the least resistance in these two tests.

Electrochemical Degradation

Electrochemical degradation tests have been performed on the four mat compositions studied in this program. These tests were performed by passing an electrolytic current of 40 ASF through the mat while it was immersed between platinum electrodes in KOH at 100°C. The tests were carried out for a duration of 72 hours. The details of the experimental procedure were as described in the Task 1 Summary Report on this program.

None of these tests showed any obvious contamination of either the electrolyte or of the electrodes. The only indication noted was a light gray deposit on the cathode during the testing of the PKT mat. In all other tests, the electrodes remained clean and bright.

Spectrographic analysis of the electrolyte and electrode wash solutions must still be completed in an attempt to identify any possible trace contaminants attributable to the mat material being tested.

TABLE 8

Liquid Permeability

Specimen	Thickness (inch)	Average Flow Time (sec.)*
Zirconia E - Chrysotile	.020"	Too rapid to measure
	.060"	14.7
Potassium Titanate PKT-Chrysotile	.020"	9.1
	.060"	36.5
Titanium Oxide - Chrysotile	.020"	52.9
	.060"	168.7
Ceric Oxide - Chrysotile	.020"	5.8
	.060"	42.8

* Time required to flow 1.12ml of water through a 1/2" diameter circular area of mat at an average head of 119.4 cm of water.

VII   CONCLUDING REMARKS

Some of the salient observations made on the suitability of various candidate materials for use in alkaline cell separators are as follows:

1. Materials that are inherently reactive with alkalis to form soluble or gaseous products will not survive long contact with KOH solutions. The natural asbestoses, being silicates are destroyed by KOH. Boron nitride reacts with KOH to generate ammonia and the reaction is accelerated by the large reactive surface area of the fibers. Silicon carbide also dissolves in KOH, probably forming hydrocarbon gas.

2. Titania and potassium titanate both react slowly with KOH at elevated temperatures to form insoluble materials, probably hydrated potassium titanate. It is possible that the hydrated material is superior to the parent material as a matrix.

3. Zirconia E is apparently essentially unchanged by long contact with hot KOH. The fibers are stiff and fragile, and consequently, mats of Zirconia E fiber have poor gas sealing properties.

4. Ceria powder is essentially unchanged by long contact with hot KOH solution. However, it has no fibrous character and, therefore, requires a fiber addition to provide coherence and gas sealing properties when saturated.

The mats made from titania, PKT, zirconia, and ceria showed some promise of improvement over the Fuel Cell Grade Asbestos mats evaluated in Task 1 of the program. The main advantage of these mats is their improved chemical compatibility with the electrolyte compared to the asbestos mats. Their electrolyte absorption and retention properties are generally as good as the asbestos mats (some are not as good and some are better). Another significant area of improvement is their lower resistance to electrolytic conduction.

In certain other properties, these mats are inferior to asbestos. One such property of importance is the bubble pressure. However, these mats may have adequate bubble pressure when they can retain their structural integrity. This bubble pressure consideration helps emphasize the main shortcoming of these

mats which is their loss of structural integrity when saturated with electrolyte. It seems this is the central problem that must be overcome to allow these materials to be useful in improved separator mats. (One additional consideration is that these specific mats contained 10% chrysotile asbestos fibers, therefore, they would not completely overcome the inherent shortcomings of the asbestos even if they were satisfactory in all other respects.)

The key to developing improved separators using these four promising materials (titania, PKT, ceria, and zirconia) seems to be in finding a way to eliminate any asbestos in the mats and yet improve their structural integrity.

One possible approach suggested by the results of this program for using titania and/or PKT is to allow porous structures of these materials to react with KOH at high temperatures to form a hydrated structure and, by so doing, possibly improve the mechanical properties of the original structure. Perhaps some exploratory studies to check on the feasibility of this approach should be undertaken.

Another approach is to develop these materials in improved fiber forms. Fiber technology is advancing rapidly, and this may soon be a technologically and economically feasible approach. Potassium titanate, for example, had been available in a more fibrous form as "Tipersul", but there was apparently insufficient economic justification for maintaining a producing capability for this material. The technology for producing such fibers, however, is obviously available.

A more expedient approach for the present, and one that is applicable to any of these materials, is to find a suitable and available fiber or other reinforcing system to render structural integrity to mats made from these promising materials. For such reinforcing materials, we must turn to the organic polymers. Even here we are limited by temperature requirements. However, the fluorinated hydrocarbons appear to have the necessary combination of temperature capability and chemical inertness for use in this application. Polypropylene also seems promising for the lower temperature applications.

The organic-polymer-reinforcement system is, in fact, the approach scheduled for the follow-on work on this program. Various combinations of these promising inorganic materials will be composited with various types and forms of organic fibers and binders as an approach toward obtaining a really suitable cell separator material.

DISTRIBUTION LIST

National Aeronautics and Space Administration
Washington, D. C.   20546
Attention: Ernst M. Cohn, Code RNW
             T. Albert, Code MLT
             A. M. Andrus, Code FC
             A. L. Inglefinger

National Aeronautics and Space Administration
Scientific and Technical Information Facility
Post Office Box 33
College Park, Maryland   20740
Attention: NASA Representative
(2 Copies plus 1 Reproducible)

National Aeronautics and Space Administration
Goddard Space Flight Center
Greenbelt, Maryland 20711
Attention: Thomas Hennigan, Code 716. 2

National Aeronautics and Space Administration
Langley Research Center
Langley Station
Hampton, Virginia   23365
Attention: S. T. Peterson

National Aeronautics and Space Administration
Lewis Research Center
21000 Brookpark Road
Cleveland, Ohio   44135
Attention: B. Lubarsky, MS 500-201
             H. J. Schwartz, MS 500-201
             J. E. Dilley, MS 500-309
             N. D. Sanders, MS 302-1
             Dr. J. S. Fordyce, MS 302-1
             V. Hlavin, MS 3-14 (Final Only)
             Technology Utilization Office, MS 3-19
             D. G. Soltis, MS 500-202
             Library, MS 60-3
             Report Control, MS 5-5
             M. R. Unger, MS 500-201

National Aeronautics & Space Administration
Marshall Space Flight Center
Huntsville, Alabama   35812
Attention: Mr. Charles Graff
            R-ASTR-EAP

National Aeronautics & Space Administration
Marshall Space Flight Center
Huntsville, Alabama   35812
Attention: Mr. Richard Boehme
            R-ASTR-E

National Aeronautics & Space Administration
Ames Research Center
Moffett Field, California 94035
   Mountain View
Attention: James R. Swain

National Aeronautics & Space Administration
Ames Research Center
Moffett Field, California   94035
   Mountain View
Attention: Mr. T. Wydeven, Environmental Control Branch

National Aeronautics & Space Administration
Ames Research Center
Moffett Field, California   94035
   Mountain View
Attention: John Rubenzer

National Aeronautics & Space Administration
Manned Spacecraft Center
Houston, Texas 77001
Attention: William R. Dusenbury
            Robert Cohen, Gemini Project Office
            F. E. Eastman (EE-4)
            Hoyt McBryar, EP-5, Bldg. 16

Jet Propulsion Laboratory
4800 Oak Grove Drive
Pasadena, California   91103
Attention: Aiji Uchiyama

Department of the Army

U.S. Army Engineer R&D Labs.
Fort Belvoir, Virginia 22060
Attention: Dr. Galen Frysinger (Code SMOFB-EP)
            Electrical Power Branch

U.S. Army Electronics R&D Labs.
Fort Monmouth, New Jersey 07703
Attention: Code SELRA/SL-PS

Harry Diamond Labs.
Room 300, Building 92
Connecticut Avenue & Van Ness Street, N.W.
Washington, D.C. 20008
Attention: Nathan Kaplan

Army Material Command
Research Division
AMCRD-RSCM T-7
Washington, D.C. 20012
Attention: John W. Crellin
           Marshall Aiken

Natick Labs.
Clothing & Organic Materials Division
Natick, Massachusetts 01760
Attention: Leo A. Spano
            Robert N. Walsh

U.S. Army TRECOM
Physical Sciences Group
Fort Eustis, Virginia 23604
Attention: (SMOFE)

U.S. Army Research Office
Box CM, Duke Station
Durham, North Carolina 27706
Attention: Paul Greer
            Dr. Wilhelm Jorgensen

U.S. Army Mobility Command
Research Division
Center Line, Michigan 48015
Attention: O. Renius (AMSMO-RR)

Department of the Air Force

Flight Vehicle Power Branch
Air Force Aero Propulsion Laboratory
Wright-Patterson Air Force Base, Ohio 45433
Attention: Don R. Warnock (Code APIP-2)

Air Force Cambridge Research Laboratory
Attention: CRZE
L. C. Hanscom Field
Bedford, Massachusetts 01731
Attention: Code CRFE

Rome Air Development Center
Griffiss AFB, New York 13442
Attention: Frank J. Mollura (EMEAM)

Lt. L. S. Harootyan
Energy Conversion Branch
Aero-Propulsion Laboratory
Wright-Patterson Air Force Base, Ohio 45433

Mr. Jesse Crosby, MAMP
Air Force Materials Laboratory
Wright-Patterson Air Force Base, Ohio 45433

Atomic Energy Commission

Army Reactors, DRD
U. S. Atomic Energy Commission
Washington, D. C. 20545
Attention: D. B. Hoatson

Department of the Navy

Office of Naval Research
Department of the Navy
Washington, D. C.   20360
Attention: Dr. Ralph Roberts, Code 429

Office of Naval Research
Department of the Navy
Washington, D. C.   20360
Attention: H. W. Fox, Code 425

Bureau of Naval Weapons
Department of the Navy
Washington, D. C. 20360
Attention: Milton Knight, Code RRRE-62

U. S. Naval Research Laboratory
Washington, D. C.   20390
Attention: Dr. J C. White, Code 6160

Bureau of Ships
Department of the Navy
Washington, D. C. 20360
Attention: C. F. Viglotti, Code 660

Naval Ordance Laboratory
Department of the Navy
Corona, California 91720
Attention: William C. Spindler (Code 441)

Naval Ordnance Laboratory
Department of the Navy
Silver Springs, Maryland 20910
Attention: Phillip B. Cole (Code WB)

U. S. Navy Marine Engineering Laboratory
Special Projects Division
Annapolis, Maryland 21402
Attention: J. H. Harrison

TRW EQUIPMENT LABORATORIES

Other Government Agencies

Office, DDR&E: USW & BSS
The Pentagon
Washington, D. C. 20301
Attention: G. B. Wareham

Staff Metallurgist
Office, Director of Metallurgy Research
Bureau of Mines
Interior Building
Washington, D. C. 20240
Attention: Kenneth S. Higbie

Mr. D. Bienstock
Bureau of Mines
4800 Forbes Avenue
Pittsburgh, Pennsylvania   15213

Office of Technical Services
Department of Commerce
Washington, D. C.   20009

Clearing House
5285 Park Royal Road
Springfield, Virginia 22151

Private Industry

Aeronutronic Division
Philco Corporation
Ford Road
Newport Beach, California 92663
Attention: Dr. S. W. Weller

Alfred University
Alfred, New York 14802
Attention: Prof. T. J. Gray

Allis-Chalmers Mfg. Company
1100 South 70th Street
Milwaukee, Wisconsin 53201
Attention: Dr. W. Mitchell, Jr.

Allison Division
General Motors Corporation
Indianapolis, Indiana 46206
Attention: Dr. Robert B. Henderson

American Machine & Foundry
689 Hope Street
Springdale, Connecticut 06879
Attention: Dr. L. H. Shaffer
             Research & Development Division

American Cyanamid Company
1937 W. Main Street
Stamford, Connecticut 06901
Attention: Dr. R. G. Haldeman

Aerospace Corporation
P. O. Box 95085
Los Angeles, California 90045
Attention: Tech. Library Document Ctr.

Arthur D. Little, Inc.
Acorn Park
Cambridge, Massachusetts 02140

Atlantic Refining Company
500 South Ridgeway Avenue
Glenolden, Pennsylvania 19036
Attention: Dr. Harold Shalit

Atomics International Division
North American Aviation, Inc.
8900 DeSoto Avenue
Canoga Park, California 91304
Attention: Dr. H. L. Recht

Battelle Memorial Institute
505 King Avenue
Columbus, Ohio 43201
Attention: Dr. C. L. Faust

Bell Telephone Laboratories, Inc.
Murray Hill, New Jersey 07971
Attention: Mr. U. B. Thomas

ChemCell Inc.
3 Central Avenue
East Newark, New Jersey 07029
Attention: Mr. Peter D. Richman

Clevite Corporation
Mechanical Research Division
540 East 105th Street
Cleveland, Ohio 44108

Douglas Aircraft Company, Inc.
Astropower Laboratory
2121 Campus Drive
Newport Beach, California 92663
Attention: Dr. Carl Berger

Electrochimica Corporation
1140 O'Brien Drive
Menlo Park, California 94025
Attention: Dr. Morris Eisenberg

Electro-Optical Systems, Inc.
300 North Halstead Street
Pasadena, California 91107
Attention: M. Kline

Englehard Industries, Inc.
497 Delancy Street
Newark, New Jersey 07105
Attention: Dr. J. G. Cohn

Esso Research and Engineering Company
P. O. Box 8
Linden, New Jersey 07036
Attention: Dr. C. E. Heath

The Franklin Institute
Philadelphia, Pennsylvania 19105
Attention: Mr. Robert Goodman

Garrett Corporation
1625 Eye Street, N. W.
Washington, D. C. 20013
Attention: Mr. Bowler

General Dynamics/Convair
P. O. Box 1128
San Diego, California 92112
Attention: Mr. R. W. Antell
            Electrical Sys. Dept. 549-6

General Electric Company
Direct Energy Conversion Operations
Lynn, Massachusetts 01901
Attention: Dr. H. Maget

General Electric Company
Research Laboratory
Schenectady, New York 12301
Attention: Dr. H. Liebhafsky

General Motors Corporation
Box T
Santa Barbara, California 93102
Attention: Dr. C. R. Russell

Globe-Union, Inc.
900 East Keefe Avenue
Milwaukee, Wisconsin 53201

Hughes Research Laboratories Corp.
3011 Malibu Canyon Road
Malibu, California 90265
Attention: T. M. Hahn

Ionics, Incorporated
152 Sixth Street
Cambridge, Massachusetts 02142
Attention: Dr. Werner Glass

Institute for Defense Analyses
Research & Engineering Support Div.
400 Army Navy Drive
Arlington, Virginia 22202
Attention: Dr. George C. Szego
            Dr. R. Briceland

Institute of Gas Technology
State and 34th Streets
Chicago, Illinois 60616
Attention: Dr. B. S. Baker

Johns Hopkins University
Applied Physics Laboratory
8621 Georgia Avenue
Silver Spring, Maryland 20910
Attention: W. A. Tynan

Mr. J. S. Parkinson
Johns-Manville R & E Center
P. O. Box 159
Manville, New Jersey 08835

Leesona Moos Laboratories
Lake Success Park
Community Drive
Great Neck, New York 11020
Attention: Dr. A Moos

McDonnell Aircraft Corporation
Attention: Project Gemini Office
P. O. Box 516
St. Louis, Missouri 63166

Midwest Research Institute
425 Volker Boulevard
Kansas City, Missouri 64110
Attention: Dr. B. W. Beadle

Monsanto Research Corporation
Boston Laboratories
Everett, Massachusetts 02149
Attention: Dr. J. O. Smith

Monsanto Research Corporation
Dayton Laboratory
Dayton, Ohio 44221
Attention: Librarian

North American Aviation Company
S & ID Division
Downey, California 90241
Attention: Dr. James Nash

Oklahoma State University
Stillwater, Oklahoma 74075
Attention: Prof. William L. Hughes
School of Electrical Eng.

Power Information Center
University of Pennsylvania
Moore School Building
200 South 33rd Street
Philadelphia, Pennsylvania 19104

Pratt and Whitney Aircraft Division
United Aircraft Corporation
East Hartford, Connecticut 06108
Attention: Librarian

Radio Corporation of America
Astro Division
Hightstown, New Jersey 08520
Attention: Dr. Seymour Winkler

Rocketdyne
6633 Canoga Avenue
Canoga Park, California 91304
Attention: Library, Dept. 586-306

TRW Systems
One Space Park
Redondo Beach, California 90278
Attention: Dr. A. Krausz

Speer Carbon Company
Research & Development Laboratories
Packard Road at 47th Street
Niagara Falls, New York 14304

Stanford Research Institute
820 Mission Street
So. Pasadena, California 91108
Attention: Dr. Fritz Kalhammer

Texas Instruments, Inc.
13500 North Central Expressway
Dallas, Texas 75222
Attention: Dr. Issac Trachtenberg

Thiokol Chemical Corporation
Reaction Motors Division
Denville, New Jersey 07834
Attention: Dr. D. J. Mann

TRW, Inc.
23555 Euclid Avenue
Cleveland, Ohio 44117
Attention: Librarian

Tyco Laboratories, Inc,
Bear Hill
Hickory Drive
Waltham, Massachusetts 02154
Attention: W. W. Burnett

Unified Science Associates, Inc.
826 South Arroyo Parkway
Pasadena, California 91105
Attention: Dr. Sam Naiditch

Union Carbide Corporation
12900 Snow Road
Parma, Ohio 44129
Attention: Dr. George E. Evans

University of California
Space Science Laboratory
Berkely, California 94701
Attention: Prof. Charles W. Tobias

University of Pennsylvania
Electrochemistry Laboratory
Philadelphia, Pennsylvania 19104
Attention: Prof. John O'M. Bockris

University of Pennsylvania
Philadelphia, Pennsylvania 19104
Attention: Dr. Manfred Altman

The Western Company
Suite 802, RCA Building
Washington, D. C. 20006
Attention: R. T. Fiske

Western Reserve University
Cleveland, Ohio 44101
Attention: Prof. Ernest Yeager

Westinghouse Electric Corporation
Research and Development Center
Churchill Borough
Pittsburgh, Pennsylvania 15235
Attention: Dr. A. Langer

Whittaker Corporation
Power Sources Division
9601 Canoga Avenue
Chatsworth, California 91311
Attention: Dr. M. Shaw

Yardney Electric Corporation
New York, New York 10001
Attention: Dr. George Dalin

General Motors Corporation
Research Laboratories
Electrochemistry Department
12 Mile & Mound Roads
Warren, Michigan 48090
Attention: Mr. Seward Beacom

G. M. Defense Research Lab.
P. O. Box T
Santa Barbara, California 93102
Attention: Dr. Smatko

University of Toledo
Toledo, Ohio 43606
Attention: Albertine Krohn